 CMES, vol.83, no.2, pp.169-181, 2012

Comparison between a Cohesive Zone Model and a Continuum Damage Model in Predicting Mode-I Fracture Behavior of Adhesively Bonded Joints

K.I. Tserpes[1] **and A.S. Koumpias**[1]

Abstract: In this work, a comparison between a cohesive zone model and a continuum damage model in predicting the mode-I fracture behavior of adhesively bonded joints is performed on the basis of reliability and applicability. The cohesive zone model (CZM) is based on an exponential traction law characterizing the behavior of the interface elements. The continuum damage model (CDM) is based on the stiffness degradation of adhesive elements imposed by a damage parameter. Both models have been implemented by means of a 3D finite element model. Mode-I fracture behavior of the bonded joints was characterized using the DCB specimen. Firstly, the models were validated satisfactorily through the simulation of a metallic bonded joint for which numerical results exist in the literature. To compare the models, an adhesively bonded joint between CFRP plates, for which in-house experimental results were available, was simulated. The comparison shows that the two models are equally reliable as they implement a similar theory. Nevertheless, the predictions of the CDM show a greater dependency on the mesh density and load increment than the CZM. Furthermore, implementation of the CDM requires five input parameters, some of which are experimental, whereas implementation of the CZM requires two input parameters which can be derived from the material properties of the adhesive. A disadvantage of the CZM is the increased computational time attributed to the time-consuming non-linear analysis.

Keywords: Bonded joints, Adhesive, Continuum damage, Cohesive zone modeling, Finite elements.

1 Introduction

The use of adhesive bonding for joining CFRP aeronautical structures is driven by the need for strong and lightweight structures. An optimal use of this joining technology can lead to weight savings up to 15% for the fuselage airframe which would

[1] Laboratory of Technology & Strength of Materials, University of Patras, Patras, 26500, Greece

have further effects on the size and weight of the engines. From the achieved weight savings expected are reductions in fuel consumption, and hence CO_2 emissions per passenger-kilometer, as well as in aircraft direct operating costs. Although adhesively bonded joints have many advantages over other structural joining methods, mainly related to their efficient load transfer in thin components and structural repairs, their general application has suffered due to the difficulty in inspecting bondline quality following manufacture and in-service life (Butkus and Johnson, 1998) and sensitivity of bondline integrity to environmental attack and physico-chemical conditions of the substrates.

The effort to increase the strength of composite bonded joints comprises: mechanical testing to assess the parameters affecting strength of the joints, extended and classical non-destructive techniques to monitor the quality of the bondline as well as numerical modeling for design and optimization purposes. Joint strength prediction models are based on a) classical strength of materials theory, b) fracture mechanics and c) a combination of them. Usually, the models in the first category use a stress or a strain-based failure criterion (e.g. Harris and Adams, 1984; Crocombe et al, 1990; Czarnocki and Piekarski, 1986; Tserpes et al, 2011a; Tserpes et al, 2011b), while the fracture mechanics models are based on energetic criteria (e.g. Hamaush and Ahmad, 1989; Anderson et al., 1988; Fernlund et al, 1994), such as the comparison of the energy release rates with their critical values. However, the accuracy of energetic criteria is highly dependent on the critical strain release rates of the adhesive joints.

In the last few years, the cohesive zone modeling approach is used increasingly due to its ability to simulate the entire debonding process (initiation and progression) and its ease of implementation as it has been incorporated in many commercial FE codes. The main disadvantage of this approach is the requirement for calibration of the input parameters needed due to deviation of the theoretical from the actual material properties of the adhesive. Moreover, there are some convergence difficulties arising during the Newton-Raphson non-linear solution of the softening process, which mainly occur at cases under mode-II (sliding) loading conditions. Alternatively to the cohesive zone modeling approach, the continuum damage approach has been proposed recently. The latter approach implements exactly the same theory with the cohesive zone modeling but without any convergence difficulties since it controls the softening process just by modifying the stiffness of the adhesive elements. This is a very stable and established technique taken from the classical progressive damage modeling technique.

In this work, a comparison of the effectiveness of a CZM and CDM in predicting mode-I fracture behavior of adhesively bonded joints is performed aiming to provide useful information to the reader that has to decide which modeling approach

to use for predicting strength and optimizing adhesively bonded joints.

2 Problem statement

To compare the performance of the two modeling approaches in predicting the mode-I fracture behavior of composite bonded joints, the problem of the double cantilever beam (DCB) loaded in normal tension has been considered. For the specific load-case, it is desired to predict the normal load-normal displacement curve P-$\delta\ddot{A}$. The DCB specimen and boundary conditions are schematically described in Fig.1.

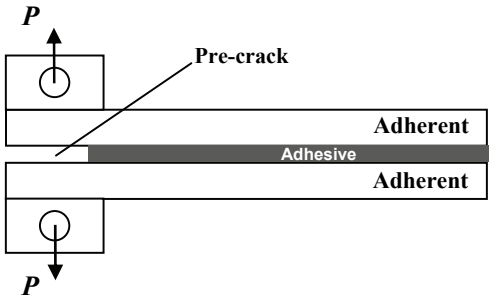

Figure 1: Schematic of the DCB specimen.

In this work, two specific cases of the DCB problem have been considered. Case 1 has been selected from de Moura and Chousal (2006) and represents a joint between metallic adherents. Case 2 represents a joint between composite CFRP (AS4/8552) adherents with layup: $[0^o/45^o/90^o/\text{-}45^o]_S$. For Case 1, there are available appropriate numerical results (continuum) for validating the two approaches, while for Case 2, there are available in-house experimental results from mode-I mechanical tests (Katsiropoulos et al, 2011) to compare the two approaches. Specimen dimensions are listed in Table 1 for both cases while material properties for Case 1 and Case 2 in Tables 2 and 3, respectively. In Case 2, the adhesive used was the FM300 K0.5 adhesive of Cytec, while in Case 2 the new aeronautical adhesive Epibond 1590 A/B from Huntsman.

3 Cohesive zone model

The CZM has been implemented by means of a 3D FE model in which the adhesive was represented using interface elements. For these elements, the interfacial

Table 1: Specimen dimensions.

Dimension	Case 1	Case 2
Specimen length (mm)	150	250
Specimen width (mm)	30	25
Adherent's thickness (mm)	1.5	1.5
Adhesive's thickness (mm)	0.25	1.0
Pre-crack length (mm)	30	25
G_{IC}(N/mm)	0.3	0.2

Table 2: Material properties for Case 1.

Property	Value
Adherent's Young's Modulus (MPa)	69000
Adherent's Poisson ratio	0.33
Adhesive's Young's Modulus (MPa)	4000
Adhesive's Poisson ratio	0.3
Adhesive's Fracture strength, σ_u(MPa)	20

Table 3: Material properties for Case 2.

Property	Value
AS4/8552	
Longitudinal Young's modulus (GPa)	141
Transverse Young's modulus (GPa)	10.0
In-plane shear modulus (GPa)	4.5
In-plane Poisson's ratio	0.3
Adhesive Epibond 1590 A/B	
Young's modulus	3000
Poisson's ratio	0.3
Adhesive's Fracture strength, σ_u(MPa)	20

separation is defined as the displacement jump,δ, i.e., the difference of the displacements of the adjacent interface surfaces (see Fig.2):

$$\delta = \mathbf{u}^{top} - \mathbf{u}^{bottom} \tag{1}$$

As shown in Fig.2, the definition of separation is based on the local element coordinate system. The normal of the interface is denoted as local direction **n**, and the

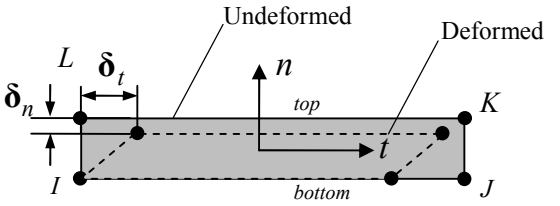

Figure 2: Schematic of interface elements.

local tangent direction is denoted as **t**. Thus:

$\delta_n = \mathbf{n} \cdot \delta$ normal separation (2)

$\delta_n = \mathbf{t} \cdot \delta$ tangential (shear) separation (3)

For describing the behavior of the interface elements, the exponential material model proposed by Xu and Needleman (1994) was adopted. The surface potential of this model is

$$\phi(\delta) = e\sigma_{\max}\bar{\delta}_n[1-(1+\Delta_n)e^{-\Delta_n}e^{-\Delta_t^2}] \tag{4}$$

where:

$\sigma_{\max}$ is the maximum normal traction at the interface,

$\bar{\delta}_n$ is normal separation across the interface where $\sigma_{\max}$ is attained with $\delta_t = 0$,

$\bar{\delta}_t$ shear separation where the maximum shear traction is attained at $\delta_t = \frac{\sqrt{2}}{2}\bar{\delta}_t$.

$\Delta_n = \frac{\delta_n}{\bar{\delta}_n}$, and

$$\Delta_t = \frac{\delta_t}{\bar{\delta}_t}.$$

The traction is defined as

$$T_n = \frac{\partial\phi(\delta)}{\partial\delta_n} \tag{5}$$

$$T_t = \frac{\partial\phi(\delta)}{\partial\delta_t} \tag{6}$$

From Eqs.(5) and (6), we get the normal traction of the interface

$$T_n = e\sigma_{\max}\Delta_n e^{-\Delta_n}e^{-\Delta_t^2} \tag{7}$$

and the shear traction

$$T_t = 2e\sigma_{\max}\frac{\bar{\delta}_n}{\bar{\delta}_t}\Delta_t(1+\Delta_n)e^{-\Delta_n}e^{-\Delta_t^2}. \tag{8}$$

The normal separation work is

$$\phi_n = e\sigma_{\max}\bar{\delta}_n \tag{9}$$

and the shear work of separation is assumed to be the same as the normal work of separations, thus

$$\phi_t = \sqrt{2}e\tau_{\max}\bar{\delta}_t. \tag{10}$$

For the 3-D stress state, the shear or tangential separations and the tractions have two components, δ_{t1} and δ_{t2} in the element's tangential plane and we have:

$$\delta_t = \sqrt{\delta_{t1}^2 + \delta_{t2}^2} \tag{11}$$

The traction is then defined as

$$T_{t1} = \frac{\partial\phi(\delta)}{\partial\delta_{t1}} \tag{12}$$

and

$$T_{t2} = \frac{\partial\phi(\delta)}{\partial\delta_{t2}}. \tag{13}$$

4 Continuum damage modeling

The CDM implemented herein is the one proposed by Moura and Chousal (2006). It is based on a bilinear softening law used also in cohesive damage models (Fig.3) which correlates adhesive failure (debonding) with stiffness degradation. This is accomplished by introducing a damage parameter d_i (element i). Stiffness degradation is related to the critical strain energy release rate G_{IC}. However, in this case a characteristic length l_c must be introduced to transform the crack opening displacement δ_n into an equivalent strain, thus the relation has the form

$$G_{IC} = \frac{1}{2}\sigma_{\max,i}\varepsilon_{u,i}l_c \tag{14}$$

where $\varepsilon_{u,i}$ is the ultimate strain at the softening process (see Fig.3) and l_c is a characteristic length transforming displacement to strain.

Under the assumption of isotropic damage evolution, degraded stiffness $E$is given by

$$E = (1 - d_i)E_0 \tag{15}$$

where the scalar parameter d_i for element i varies from 0 (undamaged adhesive) to 1 (complete debonded) and derived from

$$d_i = \frac{\varepsilon_{u,i}(\varepsilon_i - \varepsilon_{n,i})}{\varepsilon_i(\varepsilon_{u,i} - \varepsilon_{n.i})} \tag{16}$$

where ε_i is the normal strain and $\varepsilon_{n.i}$ the softening onset strain of element i (see Fig.3).

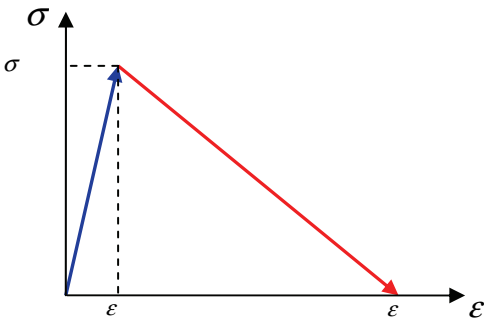

Figure 3: Softening stress-strain curve of the continuum damage model.

5 Numerical implementation

To implement both approaches, a 3D FE model of the DCB specimen has been developed using the ANSYS FE code. The adherents have been represented using the ANSYS SOLID185 element, which has also a layered option. For Case 1, an isotropic material behavior has been assigned to these elements while for Case 2 an orthotropic behavior has been assigned to represent the CFRP material. The adhesive has been represented with the ANSYS 3D INTER205 interface elements, for the CZM, and with the ANSYS SOLID185 element for the CDM. The FE mesh of the DCB specimen is shown in Fig.4. The normal tensile load has been applied in the specimen by constraining normal displacement at the nodes of the left bottom edge of the specimen and applying an incremental normal displacement at the nodes of the left top edge.

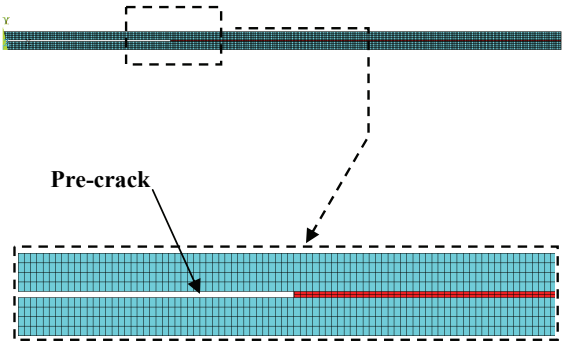

Figure 4: FE model of the DCB specimen. Red elements represent the adhesive.

In the CZM, the interface elements possess the cohesive behavior presented in section 3. In order for the cohesive zone modeling process to be implemented, it requires as input two parameters; namely, the maximum normal traction at the interface $\sigma_{\max}$, which is the σ_u and the normal separation across the interface $\bar{\delta}_n$ where $\sigma_{\max}$ is attained with $\delta_t = 0$, which was derived from the strain of debonding onset $\varepsilon_{n.i} = \sigma_u / E$ (due to the assumption of linear isotropic behavior of the adhesive) using the dimensions of the element. Therefore, the input parameters needed to implement the CZM is the σ_u and E, which are material properties of the adhesive.

The CDM has been implemented following the classical progressive damage modeling algorithm. In order for the algorithm to be implemented, it requires as input five parameters; namely, the mode-I energy release rate G_{IC}, which is derived the experimental load-displacement curve, the $\varepsilon_{n,i}$, which is taken as $\varepsilon_{n.i} = \sigma_u / E$, the l_c, which is taken equal to the length of influence of a Gauss point in the given direction (de Moura and Chousal, 2006), and $\varepsilon_{u,1}$, which is derived from Eq.(14). At every load step, the normal strain of each adhesive element ε_i is computed from the FE method and the element's stiffness is updated using Eq.(15) after having computed the parameter d_i from Eq.(16).

6 Models validation

To validate the models, Case 1 has been modeled and the computed results were compared against the continuum damage model of de Moura and Chousal (2006). The three load-displacement curves are compared in Fig.5. The load is the total reaction force measured at the constrained nodes and the displacement is the applied normal displacement. As can be seen, an excellent agreement has been achieved

between the CZM model, the CDM model and the model of de Moura and Chousal (2006) for all features of the curve (stiffness, maximum load and softening part), thus validating the models satisfactorily.

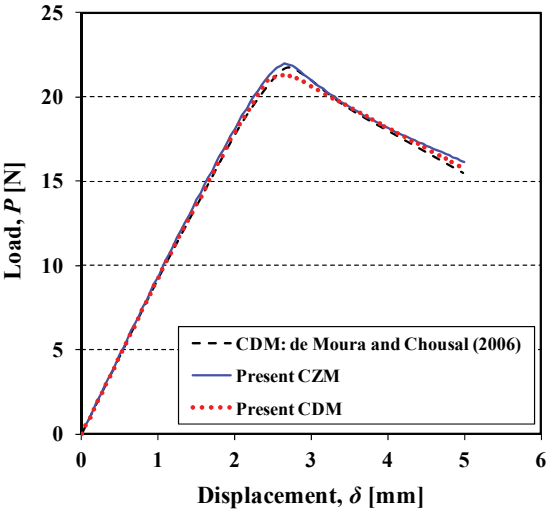

Figure 5: Comparison of load-displacement curves predicted for Case 1 with the CDM of de Moura and Chousal (2006).

7 Comparison of the models

To compare the models, we consider Case 2. For this case, the experimental load-displacement curve is available from Katsiropoulos et al. (2011). The experiment has been conducted under the specification AITM-1.0053 (2006). As an additional element of the comparison, it will be very interesting to consider, whether the two models could be applied if no experimental data are available.

Before comparing the predicted load-displacement curves with the experimental one, it is very useful to describe the process followed to apply each model.

As stated in section 3, to implement the CZM two input parameters are needed; namely, the $\sigma_{\max}$ and the $\bar{\delta}_n$. To derive them one need just the material properties of the adhesive; namely, the Young's modulus E and tensile strength σ_u. However, derivation of these parameters is not an easy task since in most cases there are several parameters altering the actual material properties of the joint from the theoretical values. In bonded joints, such parameters are the defects in the bond-line and the reduced strength of adhesive/adherent interface due to poor surface

treatment. Consequently, despite the good applicability of CZM, implementation of this approach to predict experimental results is not always an easy task. On the other hand, to implement the CDM, additional to the material properties of the adhesive, the G_{IC} and the very sensitive parameter l_c are also needed. Therefore, it is concluded that in the case of lack of experimental data, the CDM cannot be applied.

The numerical load-displacement curves for Case 2 are compared with the experimental curve in Fig.6. At the experimental curve, displacement is the one applied by the moving grip and load is the normal load measured by the steady grip. The two models give almost identical predictions as they implement a similar theory. Note that as stated previously, for the CZM, degraded values of the adhesive's material properties have been used for deriving the input parameters. On the other hand, it must be also noted, that for the curve of the CDM to be reached, several analyses with different mesh densities and load increments have been performed due to the sensitivity of the CDM algorithm on these parameters.

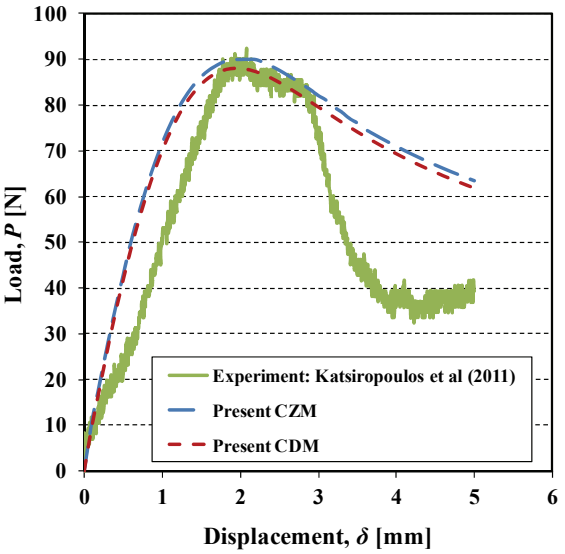

Figure 6: Comparison of load-displacement curves predicted for Case 2 with the experimental curve.

Comparison shows that the initial stiffness, the maximum load and the first part of the softening region are very well-captured by the models. The deviation at the stiffness and at the latter softening region is mainly due to the inhomogeneity of the bondline owing to the presence of defects. In general, the model predictions can be regarded accurate as they capture the overall mode-I fracture behavior of

the composite bonded joint and mainly because they capture the maximum load, which is the most important factor for the integrity of composite bonded joints, thus comprising the design factor for the joints in aeronautical applications.

Between the two models, there is also a significant difference of the consumed computational time. The CDM is more time-consuming by 50% as it implements a non-linear Newton-Raphson solution, while the CDM implements a fully adjustable non-linear solution.

Fig.7 illustrates the deformed shape of the bonded joint at the displacement of 5mm predicted by CZM. A similar deformed is obtained for the CDM. In the figure, large deformation of the adhesive due to debonding is visible.

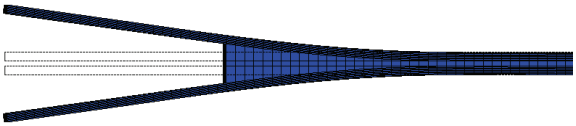

Figure 7: Predicted deformed shape of the bonded joint at the displacement of 5mm for the CZM.

8 Conclusions

In this work, a comparison of a cohesive zone model and a continuum damage model in predicting the mode-I fracture behavior of adhesively bonded joints was performed on the basis of reliability and applicability. From the findings of the paper, the following conclusions can be drawn

1. The two models are equally reliable as they implement a similar theory,
2. The predictions of the CDM show a larger dependency on the mesh density and load increment than the CZM,
3. Implementation of CDM requires five input parameters, some of which are experimental, whereas implementation of CZM requires two input parameters which can be derived from the material properties of the adhesive,
4. A disadvantage of the CZM is the increased (by 50%) computational time attributed to the time-consuming non-linear analysis,
5. Implementation of both models in bonded joints, for which experimental results are available, is difficult due to the deviation of the actual material properties of the adhesive from the theoretical values.

Aiming to complete the comparison of the CZ and CD modeling approaches, a similar study for the mode-II fracture behavior of the bonded joints is currently being accomplished by the authors.

References

AITM1-1.0053. (2006): Airbus test method: determination of fracture toughness energy of CFRP bonded joints – mode I.

Anderson, G.P.; Brinton, S.H.; Ninow, K.J.; DeVries, K.L. (1988): A fracture mechanics approach to predicting bond strength. *In: Advances in adhesively bonded joints. New York: ASME* pp. 93–101.

ANSYS Release 11.0. (2007): Documentation.

Butkus, L.M.; Johnson, W.S. (1996): *Designing for the durability of bonded structures*. FAA/NASA Symposium on Continued Airworthiness of Aircraft Structures, 28–30 August, Atlanta (GA).

Czarnocki, P.; Piekarski, K. (1986): Non-linear numerical stress analysis of a symmetric adhesive bonded lap shear joint. *International Journal of Adhesion and Adhesives*, vol. 3, pp. 157–60.

Crocombe, A.D.; Bigwood, D.A.; Richardson, G. (1990): Analyzing structural adhesive joints for failure. *International Journal of Adhesion and Adhesives*, vol. 10, pp. 167–78.

de Moura, M.F.S.F.; Chousal, J.A.G. (2006): Cohesive and continuum damage models applied to fracture characterization of bonded joints. *International Journal of Mechanical Sciences*, vol. 48, pp. 493–503.

Fernlund, G.; Papini, M.; McCammond, D.; Spelt, J.K. (1994): Fracture load predictions for adhesive joints. *Composites Science and Technology*, vol. 51, pp. 587–600.

Hamaush, S.A.; Ahmad, S.H. (1989): Fracture energy release rate of adhesive joints. *International Journal of Adhesion and Adhesives*, vol. 9, pp. 171–8.

Harris, J.A.; Adams, R.D. (1984): Strength prediction of bonded single lap joints by non-linear finite element methods. *International Journal of Adhesion and Adhesives*, vol. 4, pp. 65–78.

Katsiropoulos, Ch.V.; Chamos, A.N.; Tserpes, K.I.; Pantelakis, Sp.G. (2011): Fracture toughness and shear behavior of composite bonded joints based on a novel aerospace adhesive. *Composites Part B: Engineering*, DOI: 10.1016/j.compositesb.2011.07.010.

Tserpes, K.I.; Cinquin, J.; Pantelakis, Sp. (2011): On the mechanical performance of noncrimp fabric H-shaped adhesively bonded joints. *Journal of Composite Materials*, vol. 45, pp. 1607-1619.

Tserpes, K.I.; Pantelakis, S.; Kappatos, V. (2011): The effect of imperfect bonding on the pull-out behavior of non-crimp fabric Pi-shaped joints. *Computational Materials Science*, vol. 50, pp. 1372-1380.

Xu, X-P.; Needleman, A. (1994): Numerical simulations of fast crack growth in brittle solids. *Journal of the Mechanics and Physics of Solids*, vol. 42, pp. 1397-1434.